




This article may be downloaded for personal use only. Any other use requires prior permission of the author and AIP Publishing. This article appeared in Pancheng Zhu, Zhen Song, Stanley Sau-ching Wong, Yongping Zheng; Quantitative neuromuscular monitoring with train-of-four ratio using sonomechanomyography (SMMG): Toward more sensitive evaluation of neuromuscular blockade. *Rev. Sci. Instrum.* 1 December 2024; 95 (12): 123701 and may be found at <https://doi.org/10.1063/5.0243459>.

RESEARCH ARTICLE | DECEMBER 02 2024

## Quantitative neuromuscular monitoring with train-of-four ratio using sonomechanomyography (SMMG): Toward more sensitive evaluation of neuromuscular blockade

Pancheng Zhu ; Zhen Song; Stanley Sau-ching Wong; Yongping Zheng  



*Rev. Sci. Instrum.* 95, 123701 (2024)

<https://doi.org/10.1063/5.0243459>



### Articles You May Be Interested In

Development of 3D neuromuscular bioactuators

*APL Bioeng.* (March 2020)

Neuromuscular control of fundamental frequency and glottal posture at phonation onset

*J. Acoust. Soc. Am.* (February 2012)

Noninvasive direct assessment of the skeletal muscle function during neuromuscular electrical stimulation

*J. Acoust. Soc. Am.* (October 2021)



Think Nano® | Positioning | Microscopy | Solutions

- Nanopositioning Systems • Micropositioning Systems
- Atomic Force Microscopes • Single Molecule Microscopes
- Custom Solutions

# Quantitative neuromuscular monitoring with train-of-four ratio using sonomechanomyography (SMMG): Toward more sensitive evaluation of neuromuscular blockade

Cite as: *Rev. Sci. Instrum.* **95**, 123701 (2024); doi: [10.1063/5.0243459](https://doi.org/10.1063/5.0243459)

Submitted: 11 October 2024 • Accepted: 6 November 2024 •

Published Online: 2 December 2024



View Online



Export Citation



CrossMark

Pancheng Zhu,<sup>1</sup>  Zhen Song,<sup>1</sup> Stanley Sau-ching Wong,<sup>2</sup> and Yongping Zheng<sup>1,3,a)</sup> 

## AFFILIATIONS

<sup>1</sup> Department of Biomedical Engineering, The Hong Kong Polytechnic University, Hong Kong 999077, China

<sup>2</sup> Department of Anaesthesiology, School of Clinical Medicine, Li Ka Shing Faculty of Medicine, The University of Hong Kong, Hong Kong 999077, China

<sup>3</sup> Research Institute for Smart Ageing, The Hong Kong Polytechnic University, Hong Kong 999077, China

<sup>a)</sup> Author to whom correspondence should be addressed: [yongping.zheng@polyu.edu.hk](mailto:yongping.zheng@polyu.edu.hk)

## ABSTRACT

In the post-anesthesia care unit, there is a high occurrence of residual neuromuscular blockade, which puts patients at risk of negative consequences such as hypoxia. Assessment based on the train-of-four ratio (TOFR) has been used to avoid residual neuromuscular blockade when the TOFR is greater than 0.9, measured at the adductor pollicis muscle (APM). The most commonly used quantitative neuromuscular monitoring (QNM) modalities include acceleromyography (AMG) and electromyography (EMG). However, the poor user-friendliness of current QNM methods hinders their widespread adoption. To overcome this, we developed a new monitoring method using ultra-fast ultrasound imaging to generate a two-dimensional map of muscle transient motion, i.e., sonomechanomyography (SMMG). SMMG of the APM and AMG of the thumb were used to get the TOFR of 20 normal adults. The results showed no significant difference between the left and right hands for both AMG and SMMG TOFR, with p-values larger than 0.05. In addition, the mean accuracy of SMMG TOFR (0.6% relative error) was higher than AMG (1.4% relative error). Moreover, the Bland–Altman plot showed that all the difference values were within the limits of agreement and the mean bias was 0.02, indicating that the two methods had a very good agreement. In particular, using SMMG did not require additional calibration before testing. Overall, the results demonstrated that the method has the potential as a new QNM approach for further clinical studies to benefit patients in need. To demonstrate its clinical potential, further studies are required to evaluate this method in patients during and post-anesthesia.

Published under an exclusive license by AIP Publishing. <https://doi.org/10.1063/5.0243459>

## I. INTRODUCTION

During the administration of anesthesia, it is imperative to continuously assess the patient's physiological condition to ensure the efficacy of the anesthetic procedure. This can be accomplished through a combination of clinical observations and the use of monitoring equipment. Clinical observations include assessing the color of the mucous membranes, pupil size, and the presence of tear production.<sup>1</sup> The Association of Anaesthetists emphasizes the importance of adhering to minimum monitoring standards for all anesthetized patients, irrespective of the anesthesia's duration or

setting.<sup>1</sup> Presently, there is a notable prevalence of residual neuromuscular blockade (rNMB), which exposes patients to adverse outcomes such as hypoxemia, upper airway obstruction, aspiration, prolonged recovery in the post-anesthesia care unit (PACU), and general discomfort.<sup>2,3</sup> To mitigate these risks, vigilant monitoring of neuromuscular blockade depth is crucial when neuromuscular blocking agents (NMBAs) are utilized.

Clinical assessment traditionally serves as the primary method for evaluating a patient's recovery of strength, yet its reliability is questionable.<sup>4</sup> The peripheral nerve stimulator (PNS) emerges as a

valuable instrument, facilitating nerve stimulation that allows clinicians to assess muscle response via visual or tactile means.<sup>5</sup> Due to its convenience and user-friendly interface, PNS has gained widespread acceptance in clinical settings. Nonetheless, the subjective nature of evaluating nerve blocks through PNS represents a significant drawback, particularly as it offers less precision compared to quantitative neuromuscular monitoring (QNM) at minimal levels of the blockade.<sup>6</sup> To circumvent issues of rNMB, measuring the train-of-four ratio (TOFR) is advocated. Neuromuscular recovery is deemed satisfactory when the TOFR reaches or exceeds 0.9, specifically when measured at the adductor pollicis muscle (APM).<sup>7</sup> The TOFR stimulation protocol involves delivering four stimuli at a frequency of 2 Hz, with each stimulus spaced 0.5 s apart. The TOFR is calculated by dividing the amplitude of the fourth muscle response (T4) by that of the first muscle response (T1). Therefore, for a more accurate assessment of neuromuscular function within clinical environments, the utilization of TOFR alongside a quantitative monitoring device is recommended. This approach not only enhances the precision of evaluations but also significantly reduces the risk of complications associated with rNMB.

Currently, different QNM measurement techniques are available for TOFR assessment. Mechanomyography (MMG) is highly sensitive and often regarded as the potential “gold standard” due to its precise and reliable results. However, current MMG measurement is hindered by a cumbersome setup process, such as the need for calibration before use, and a lack of commercially available systems designed for clinical applications.<sup>8</sup> Kinemyography (KMG) features a straightforward setup that eliminates the need for an external display or calibration, but its use is limited to the APM.<sup>9</sup> Acceleromyography (AMG) offers the flexibility to be used on any muscle capable of free movement, including those in the hand, foot, or face. Nevertheless, it is not suitable for immobilized muscles, and to optimize accuracy, the device requires calibration before the administration of NMBA and normalization against baseline readings.<sup>10</sup> Electromyography (EMG) is considered as accurate and reliable as MMG and can be applied to a diverse range of locations, including immobilized muscles. However, EMG is susceptible to electrical interference, and its accuracy may be compromised by low muscle temperature. Similar to AMG, EMG also necessitates device calibration before NMBA administration to ensure high precision.<sup>11</sup> Hence, the primary obstacle to the broader implementation of QNM is not their cost but rather the challenges associated with their ease-of-use and consistency.<sup>12</sup> To address these issues, there is a need for innovative monitoring techniques that are unaffected by the patient’s hand placement, capable of self-calibration, able to deliver dependable outcomes, simple to install, and yield reproducible responses. The development of such methods would greatly facilitate the integration of QNM into routine clinical practice, enhancing patient safety and the overall quality of care in anesthesia.

Ultrasound imaging presents a superior alternative for muscle monitoring, offering a non-invasive method to evaluate muscle architecture.<sup>13</sup> Through B-mode ultrasound imaging, sonomyography (SMG) assesses dynamic muscle morphology, including thickness, pennation angle, fascicle length, and cross-sectional area.<sup>14</sup> SMG is derived from B-mode ultrasound images, which are traditionally limited to a sampling rate of ~30 f/s. However, advancements in ultrafast ultrasound imaging now permit B-mode imaging

at significantly higher frame rates, often reaching several thousand frames per second (fps).<sup>15</sup> In this research, we utilized ultrafast ultrasound imaging with a frame rate exceeding 2000 fps to generate a two-dimensional representation of transient muscle motion, termed sonomechanomyography (SMMG).<sup>16</sup> The cutting-edge SMMG technology has recently demonstrated considerable potential in enhancing our comprehension of neuromuscular disorders; for example, using this method, it was found that the use of transverse friction massage could decrease active muscle stiffness.<sup>17</sup> In addition, it offers valuable insights that aid in pinpointing changes in muscle activation timing and in evaluating the effectiveness of therapeutic interventions.<sup>16</sup> SMMG’s unique ability to measure muscle vibration from different locations within the muscle, coupled with its complementary features to existing muscle-related signals such as EMG and MMG, makes it a versatile and valuable tool for various applications. This study aims to develop a novel approach and protocol that leverages SMMG to map out muscle movements in two dimensions to achieve precise and reliable QNM during anesthesia and recovery, making it a promising technology for the future.

## II. EXPERIMENTAL SECTION

### A. Subjects

For this study, a convenient sampling strategy was employed to enlist 20 healthy individuals (7 females and 13 males) ranging in age from 18 to 52 years. Eligible subjects were required to be free of any implantable electronic devices and without a history of metabolic, neurological, or muscular diseases that could influence the outcomes of the investigation. The inclusion criteria allowed for individuals with occasional sports participation or those leading a sedentary lifestyle. However, professional athletes were excluded to avoid potential confounding factors related to enhanced neuromuscular performance. Ethical clearance for the study was granted by the Human Subjects Ethics Sub-Committee (HSESC) of The Hong Kong Polytechnic University (HSEARS20240220002), and all subjects provided written informed consent before participation. As detailed in Table I, data were gathered from the 20 participants, who had an average height of  $171.5 \pm 8.0$  cm and an average weight of  $66.5 \pm 13.6$  kg.

### B. System setup

Figure 1(a) illustrates the experimental setup for neuromuscular stimulation and ultrafast ultrasound imaging. Neuromuscular stimulation was delivered using a biphasic constant current stimulator (DS8R, Digitimer Ltd., Hertfordshire, UK). Concurrently, ultrasound images were captured with an advanced open ultrasound research platform (Verasonics Vantage 128, Verasonics, Inc., Kirkland, WA, USA). A dedicated computer managed the image

TABLE I. Subject characteristics.

Age (years) – mean (SD)	Gender (female: male)	Weight (kg) – mean (SD)	Height (kg) – mean (SD)
27 (7)	7:13	66.5 (13.6)	171.5 (8.0)

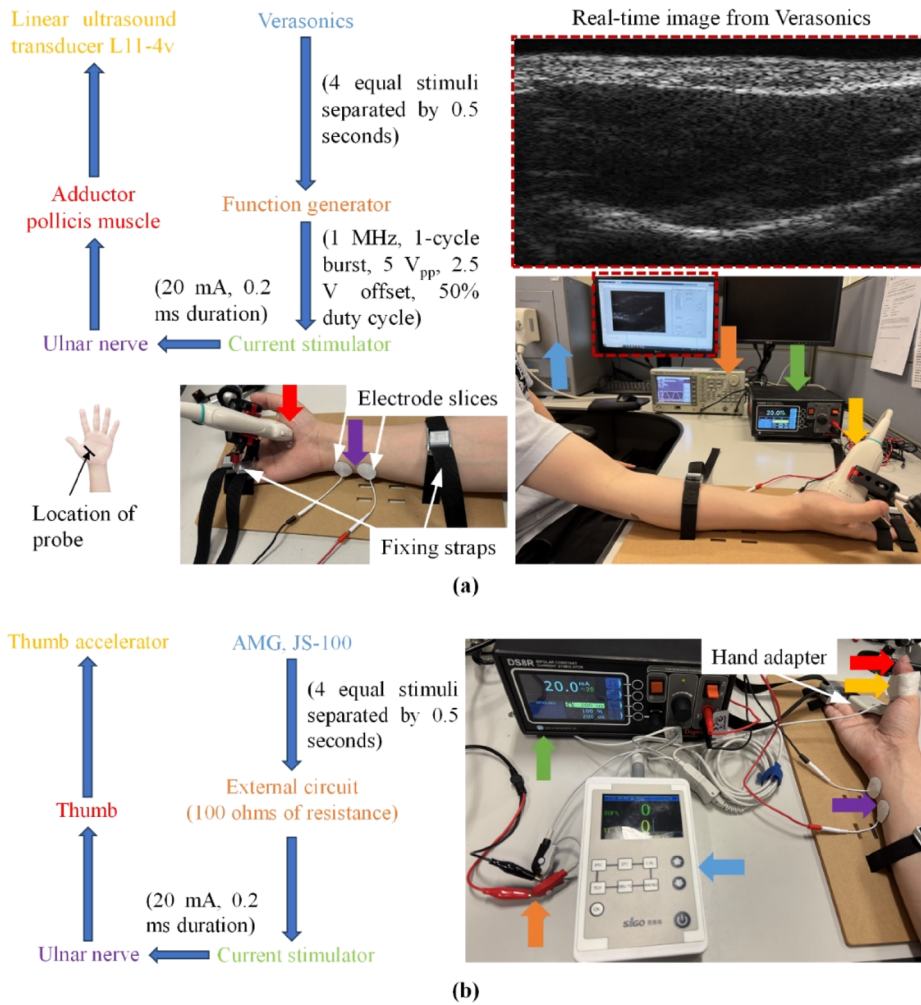


**FIG. 1.** Setup of the two devices for QNM: (a) The proposed SMMG-based QNM setup. An attachable probe is used for this purpose. (b) The AMG-based QNM setup. An accelerometer at the thumb is used for the reference signal.

acquisition process and data storage. The custom imaging script was divided into two segments: the initial segment facilitated real-time imaging by accurately positioning the broadband linear ultrasound transducer L11-4v on the APM to ensure proper location and orientation. The subsequent segment managed the trigger output to the stimulator and the data acquisition process. The transducer operated at a frame rate of 2000 Hz, capturing a sequence of 5000 frames. Upon initiating the recording, a trigger-out signal was dispatched from the Verasonics system to a function generator (AFG3052C, Tektronix, Beaverton, USA), which in turn transmitted a signal to the current stimulator (1 MHz, 1-cycle burst, 5 V<sub>pp</sub>, 2.5 V offset, 50% duty cycle). Two self-adhesive stimulation electrodes, each with a diameter of 3.2 cm (ValuTrode, Axelgaard Manufacturing Co. Ltd., USA), were employed to stimulate the ulnar nerve. The ultrasound system's radio frequency raw data were preserved for subsequent image reconstruction and analysis.

Figure 1(b) depicts the setup for QNM based on AMG. The AMG measurements were conducted using a commercial anesthesia monitoring device (JS-100, Beijing Sigo Medical Technology Co.,

LTD., China). AMG technology, grounded in Newton's Second Law of Motion (force = mass × acceleration), utilizes a piezoelectric sensor to quantify the acceleration of the thumb during muscle contractions. Notably, the minimum stimulation current threshold of the commercial AMG device is 35 mA, whereas the minimum current used in our study was 20 mA. To reconcile this discrepancy, we attenuated the stimulation current amplitude of the AMG device to 20 mA by integrating a 100-Ω resistor with the external current stimulator. This adjustment allowed the AMG device's stimulation current output to serve as the input signal for the current stimulator.

### C. Experimental procedure

As depicted in Fig. 1, participants were seated comfortably in a chair with their arms and hands secured using a custom-designed plate and straps, ensuring stability during the testing procedure. The skin was cleansed with medical alcohol to lower skin impedance to an effective range, thereby enhancing the efficacy of the electrical stimulation. Electrodes were positioned on either side of the ulnar

nerve to minimize potential errors due to nerve location variability. Subsequently, the thumb accelerometer and the SMMG probe were affixed to the thumb and palm, respectively. A specialized bracket was utilized to stabilize the ultrasound probe, ensuring that the measurement orientation remained consistently perpendicular to the APM, as illustrated in Fig. 1(a). Ultrasound gel was then applied to the APM to facilitate clear imaging. Following the instructions of the AMG anesthesia monitoring device, the accelerometer sensor for AMG was secured to the thumb using the provided hand adapter and medical adhesive tape. Participants were instructed to remain relaxed and avoid any muscle activity throughout the experiment. Each stimulation trial consisted of four identical pulses, each with a duration of 0.2 ms and an amplitude of 20 mA, spaced 0.5 s apart, in line with protocols established by previous research.<sup>18</sup> Measurements were taken five times for both the left and right hands of each subject under normal conditions, with a two-minute rest interval between each trial to prevent muscle fatigue. SMMG of the APM and AMG of the thumb were employed to determine the TOFR in the 20 healthy adults upon stimulation of the ulnar nerve. Participants might experience very mild discomfort during stimulation, comparable to sensations produced by commercially available electrical massage apparatus. Upon completion of all stimulation trials, subjects were carefully disconnected from the sensors and released from the study.

#### D. Image processing

As shown in Fig. 2, we proposed a semi-automatic algorithm to quantify muscle thickness changes in ultrafast B-mode ultrasound. The first-frame annotation of the muscle border was provided by the user, and the proposed algorithm depicted muscle thickness over time. We prepared an anonymized dataset comprising sequential ultrasound images of muscle  $I_{H \times W \times 3}$  and annotations of muscle borders  $M_{H \times W \times 1}$ , i.e., aponeurosis and tendon. A total of 1251 images from 35 sequences were collected using different devices from the gastrocnemius, diaphragm, tibialis anterior, and SMMG of the APM to enhance the variability of the dataset. The images were annotated by an experienced sonographer.

XMem,<sup>19</sup> a state-of-the-art long-term video tracking algorithm, was fine-tuned with our ultrasound dataset. Inspired by the

Atkinson–Shiffrin human memory model, XMem consists of three memory modules, namely, sensory, working, and long-term memory, which is suitable for ultrafast ultrasound images with high frame rates and long sequences. For  $t$ th ultrasound frame  $I_{H \times W \times 3}$  from the sequence, memory reading was performed to obtain memory features  $F$  representing memory key  $k$  and value  $v$  of memory. Together with the sensory memory from  $(t - 1)$ th frame, features  $F$  were fed into the decoder to generate a mask  $\hat{M}_{H \times W \times 1}$ . Memory was updated after each inference. In our task, the model was pre-trained on YouTubeVOS<sup>20</sup> and DAVIS<sup>21</sup> and fine-tuned with 15 000 iterations on a PC with an RTX 3080 GPU card. The sample  $H \times W$  size was set to  $512 \times 512$ , and the ultrasound images were scaled to a range of 0–1 before being input into the model.

In the resulting binary mask  $\hat{M}$ , the open transform was used to remove the burrs and the falsely segmented contours, presenting the main two boundaries. Assuming that the muscle boundary appeared as a linear high echo in the ultrasound image, we fitted the points on the boundary by a first-order polynomial. Finally, the mean thickness was calculated by averaging the vertical distance between two polynomials.

#### E. Data analysis

The custom script written in MATLAB (MATLAB R2020b, The MathWorks, Inc., USA) was employed to reconstruct images from the raw radio frequency ultrasound data. The data derived from image processing were subsequently analyzed using GraphPad Prism (GraphPad Prism 9.1.2, GraphPad Software, USA). All values were presented as mean  $\pm$  standard deviation (SD). A paired sample t-test was utilized to evaluate the differences between measurements obtained from the left and right hand experiments. A p-value threshold of  $>0.05$  was established to indicate a lack of statistically significant difference between the measurements of the left and right hands. Furthermore, a TOFR of 1 was adopted as the normative standard under normal physiological conditions,<sup>22</sup> and the accuracy (relative error) of measurements obtained by the two devices was calculated. In addition, the TOFR measured by AMG and SMMG were compared using Bland–Altman analysis for repeated measurements. This analysis is designed to assess the agreement between two measurement methods by evaluating the mean difference (bias)

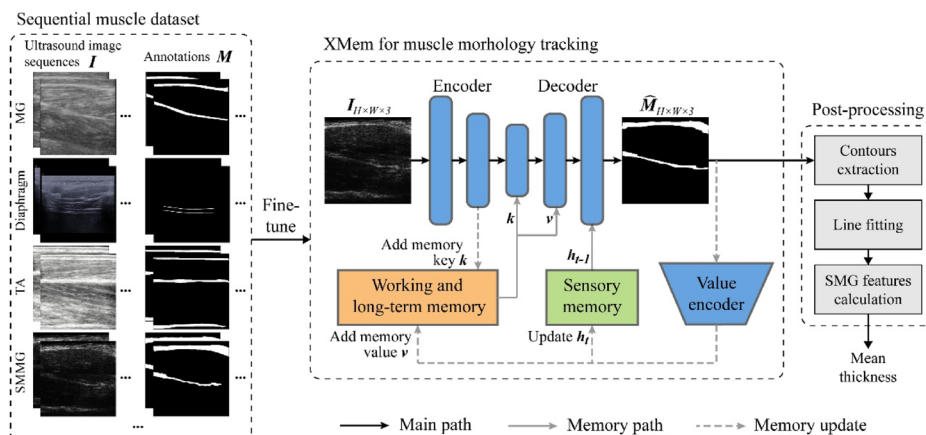


**FIG. 2.** Image processing: Quantitative muscle analysis, including multi-muscle sequence dataset for deep learning model training, XMem for muscle morphology tracking, and post-processing for SMG feature calculation.

and the 95% limits of agreement. A small bias and narrow limits of agreement are indicative of a strong agreement between the devices.

### III. RESULTS AND DISCUSSION

As depicted in Fig. 3(a), we utilized SMMG to capture a representative B-mode ultrafast ultrasound image of the APM. The average distance between the upper and lower boundaries of the muscle was selected as the measurement parameter. One of the key advantages of SMMG is its capacity for non-invasive visualization of transient muscle movements or vibrations, achieved with high spatial and temporal precision. Consequently, as illustrated in Fig. 3(b), we documented the variations in the mean thickness of the APM during a series of four identical stimuli (with 1 pixel equivalent to  $\sim 0.137$  mm). The SMMG TOFR was then determined by dividing the change in muscle thickness observed in the fourth response (T4) by that of the first response (T1), incorporating a self-calibration process. This method allows for a detailed and accurate assessment of neuromuscular function, leveraging the high frame rate capabilities of SMMG.

In the initial experiment, AMG was employed to measure the TOFR of the left and right hands of participants, as illustrated in Fig. 4. The mean AMG TOFR values for the left and right hands of the 20 subjects were  $1.016 \pm 0.016$  and  $1.011 \pm 0.035$ , respectively. Statistical analysis revealed no significant difference between the left and right hands in terms of AMG TOFR, with a p-value of 0.50 (paired t-test), which exceeds the threshold of 0.05. Concurrently, SMMG was utilized to determine the TOFR values for the subjects' left and right hands. The average SMMG TOFR values were  $0.996 \pm 0.023$  for the left hand and  $1.002 \pm 0.033$  for the right hand. Similarly, the p-value calculated for the comparison between the left and right hands was 0.55. Therefore, it can be inferred that there was no significant difference in TOFR values between the left and right hands for both AMG and SMMG, with p-values (paired t-test) exceeding 0.05. After these findings, the next phase of the experiment involved a comparative analysis of the efficacy of the AMG and SMMG methods in measuring TOFR.

Figure 5 displays the measurement outcomes of the TOFR utilizing both AMG and SMMG across 20 participants. The results reveal that the average TOFR values obtained through AMG and SMMG were  $1.014 \pm 0.021$  and  $0.994 \pm 0.018$ , respectively. Given that a TOFR of 1 was established as the normative benchmark for subjects in a normal physiological state, the mean accuracy of the SMMG TOFR was calculated to be 0.6% relative error. This accuracy surpasses that of AMG, which demonstrated a 1.4% relative error. These findings underscore the superior precision of our

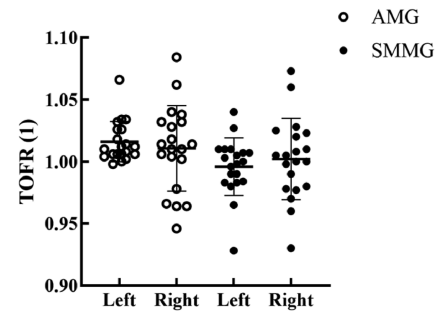


FIG. 4. Measurement of TOFR in the left and right hand using AMG and SMMG methods, respectively. No statistical significance was found.

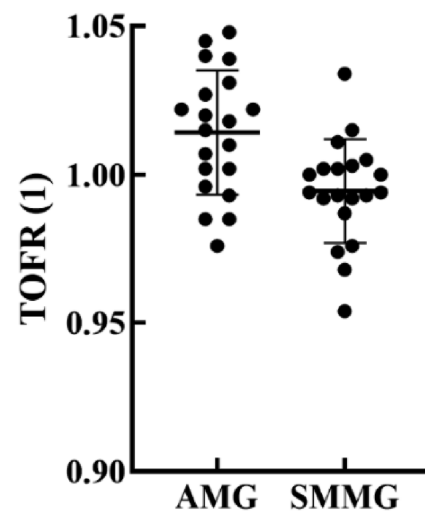


FIG. 5. Measurement results of TOFR using AMG and SMMG methods, respectively.

SMMG technique in quantifying the TOFR of subjects under normal conditions.

Figure 6 presents a Bland–Altman plot illustrating the differences in TOFR measurements obtained by AMG and SMMG plotted against their corresponding means. The plot reveals that all difference values fell within the defined narrow limits of agreement,

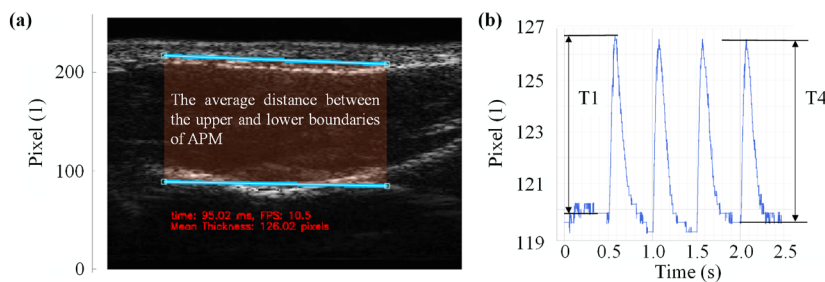
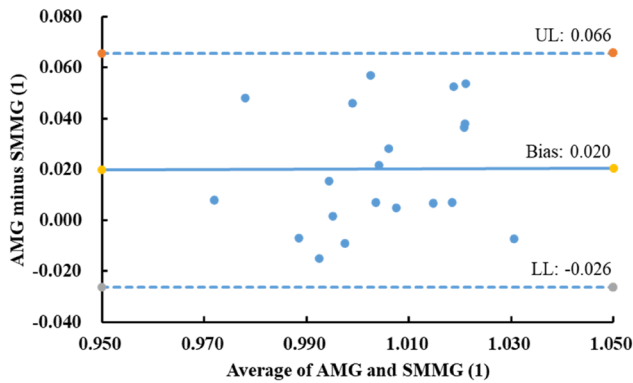


FIG. 3. SMMG TOFR: (a) A typical B-mode ultrasound image at the location of APM, and (b) the average thickness of APM varied with the number of frames under four stimuli.  $TOFR = T4/T1$ .



**FIG. 6.** Bland–Altman plot of the differences TOFR measured by AMG and SMMG against the corresponding means ( $n = 20$ ). UL = upper limit and LL = lower limit.

**TABLE II.** Agreement between different devices.

Devices	Bias	Limits of agreement	Sample size	Under anesthesia
AMG vs EMG <sup>23</sup>	0.100	-0.150–0.350	23	Y
AMG vs EMG <sup>24</sup>	0.176	-0.045–0.396	26	Y
MMG vs EMG <sup>25</sup>	0.028	-0.185–0.241	23	Y
AMG vs SMMG	0.020	-0.026–0.066	20	N

ranging from  $-0.026$  to  $0.066$ . In addition, we observed a mean difference (bias) of  $0.020$  between the TOFR measurements by AMG and SMMG, indicating that the TOFR values measured by AMG were generally higher than those measured by SMMG. When compared with biases and limits of agreement reported in other studies, as summarized in Table II, both the bias and the agreement parameters for SMMG and AMG were superior to those of other devices with a similar number of tested subjects. Consequently, we can infer that these two methods demonstrate good agreement when assessing subjects in a normal, non-anesthetized state. It is important to note that the aforementioned experiments were conducted with subjects in a non-anesthetized condition. To draw more comprehensive conclusions, clinical tests under anesthesia are required, which will form the focus of our subsequent research endeavors. This future work will aim to validate the effectiveness and reliability of this monitoring method in a clinical anesthetic context.

#### IV. CONCLUSIONS

In this research, we have successfully developed a novel QNM technique utilizing SMMG. This method involves calculating the TOFR by dividing the APM's thickness change at the fourth stimulus by that at the first stimulus, with the process being self-calibrated. We applied SMMG to the APM and AMG to the thumb to determine the TOFR in 20 healthy adults upon ulnar nerve stimulation. Our experimental findings indicated no significant differences in TOFR measurements between the left and right hands, whether using AMG or SMMG. Furthermore, we compared the SMMG

method under normal conditions with traditional anesthesia monitoring techniques, i.e., AMG, and discovered that SMMG offers superior accuracy in measuring TOFR. In addition, Bland–Altman plot analysis revealed a strong agreement between our SMMG device and the commercial AMG device. However, anesthesia can affect various physiological parameters, including muscle tone, reflexes, and overall neural activity, which can, in turn, impact the measurements obtained from devices. Hence, the presence of anesthesia is likely to influence both the bias and limits of agreement in device comparisons. Our next research plans include reducing the overall size of the whole device and designing customized fixtures to enable the entire system to be used in clinical trials, achieving the measurement of TOFR when the patient is under anesthesia.

Accurate and user-friendly monitoring of anesthesia levels and the recovery process is of paramount importance in clinical settings. The outcomes of this study imply that the system we have developed holds promise as a medical device that could enhance patient care. Nonetheless, additional research is required to assess this new method in patients during and post-anesthesia to fully ascertain its clinical applicability and efficacy.

#### ACKNOWLEDGMENTS

This work was supported by the H. G. Leong Endowed Professorship in Biomedical Engineering (Grant No. 847L) and the Postdoc Matching Fund Scheme of The Hong Kong Polytechnic University (Grant No. 1-W31W).

#### AUTHOR DECLARATIONS

##### Conflict of Interest

The authors have no conflicts to disclose.

##### Ethics Approval

Ethics approval for experiments reported in the submitted manuscript on animal or human subjects was granted. Ethical clearance for the study is granted by the Human Subjects Ethics Sub-Committee (HSESC) of The Hong Kong Polytechnic University (HSEARS20240220002), and informed consent is obtained from all participants.

##### Author Contributions

**Pancheng Zhu:** Conceptualization (equal); Investigation (equal); Methodology (equal); Project administration (equal); Validation (equal); Writing – original draft (equal). **Zhen Song:** Investigation (equal); Software (equal). **Stanley Sau Ching Wong:** Writing – review & editing (equal). **Yongping Zheng:** Conceptualization (equal); Funding acquisition (equal); Supervision (equal); Writing – review & editing (equal).

##### DATA AVAILABILITY

The data that support the findings of this study are available from the corresponding author upon reasonable request.

## REFERENCES

- <sup>1</sup>D. N. Lucas, R. Russell, J. H. Bamber, and C. D. Elton, "Recommendations for standards of monitoring during anaesthesia and recovery 2021," *Anaesthesia* **76**(10), 1426–1427 (2021).
- <sup>2</sup>S. R. Thilen, W. A. Weigel, M. M. Todd, R. P. Dutton, C. A. Lien, S. A. Grant, J. W. Szokol, L. I. Eriksson, M. Yaster, M. D. Grant, M. Agarkar, A. M. Marbella, J. F. Blanck, and K. B. Domino, "2023 American society of anesthesiologists practice guidelines for monitoring and antagonism of neuromuscular blockade: A report by the American society of anesthesiologists task force on neuromuscular blockade," *Anesthesiology* **138**(1), 13–41 (2023).
- <sup>3</sup>C. Munsterman, T. Broussard, and P. Strauss, "Botulinum toxin A injection and perianesthesia neuromuscular monitoring: Case report and review," *J. PeriAnesth. Nurs.* **37**(1), 11–18 (2022).
- <sup>4</sup>M. Naguib, S. J. Brull, A. F. Kopman, J. M. Hunter, B. Fülesdi, H. R. Arkes, A. Elstein, M. M. Todd, and K. B. Johnson, "Consensus statement on perioperative use of neuromuscular monitoring," *Anesth. Analg.* **127**(1), 71 (2018).
- <sup>5</sup>B. L. Olesnicky, A. Lindberg, F. B. Marroquin-Harris, and K. Ren, "A survey of current management of neuromuscular block and reversal in Australia and New Zealand," *Anaesth. Intens. Care* **49**(4), 309–315 (2021).
- <sup>6</sup>A. F. Kopman, P. S. Yee, and G. G. Neuman, "Relationship of the train-of-four fade ratio to clinical signs and symptoms of residual paralysis in awake volunteers," *Anesthesiology* **86**(4), 765–771 (1997).
- <sup>7</sup>M. Blobner, M. W. Hollmann, M. M. Luedi, and K. B. Johnson, "Pro-con debate: Do we need quantitative neuromuscular monitoring in the era of sugammadex?," *Anesth. Analg.* **135**(1), 39–48 (2022).
- <sup>8</sup>F. E. Blum, A. R. Locke, N. Nathan, J. Katz, D. Bissing, M. Minhaj, and S. B. Greenberg, "Residual neuromuscular block remains a safety concern for perioperative healthcare professionals: A comprehensive review," *J. Clin. Med.* **13**(3), 861 (2024).
- <sup>9</sup>C. Motamed, M. Demiri, and N. Colegrave, "Comparison of train of four measurements with kinemyography NMT DATEX and accelerography TOF scan," *Med. Sci.* **9**(2), 21 (2021).
- <sup>10</sup>A. F. Kopman, W. Chin, and J. Cyriac, "Acceleromyography vs. electromyography: An ipsilateral comparison of the indirectly evoked neuromuscular response to train-of-four stimulation," *Acta Anaesthesiol. Scand.* **49**(3), 316–322 (2005).
- <sup>11</sup>M. M. Todd, B. J. Hindman, and B. J. King, "The implementation of quantitative electromyographic neuromuscular monitoring in an academic anesthesia department," *Anesth. Analg.* **119**(2), 323 (2014).
- <sup>12</sup>L. H. Smith and L. J. Hargrove, "Comparison of surface and intramuscular EMG pattern recognition for simultaneous wrist/hand motion classification," in *2013 35th Annual International Conference of the IEEE Engineering in Medicine and Biology Society, (EMBC) (IEEE, 2013)*, pp. 4223–4226.
- <sup>13</sup>B. Van Hooren, P. Teratsias, and E. F. Hodson-Tole, "Ultrasound imaging to assess skeletal muscle architecture during movements: a systematic review of methods, reliability, and challenges," *J. Appl. Physiol.* **128**(4), 978–999 (2020).
- <sup>14</sup>Y. P. Zheng, M. M. F. Chan, J. Shi, X. Chen, and Q. H. Huang, "Sonomyography: Monitoring morphological changes of forearm muscles in actions with the feasibility for the control of powered prosthesis," *Med. Eng. Phys.* **28**(5), 405–415 (2006).
- <sup>15</sup>M. Tanter and M. Fink, "Ultrafast imaging in biomedical ultrasound," *IEEE T. Ultrason. Ferr.* **61**(1), 102–119 (2014).
- <sup>16</sup>Y. T. Ling, C. Z. H. Ma, Q. T. K. Shea *et al.*, "Mapping of skeletal muscle motion onset during contraction using ultrafast ultrasound imaging and multiple motion sensors," *Sensors* **20**(19), 5513 (2020).
- <sup>17</sup>H. Begovic, G.-Q. Zhou, S. Schuster, and Y.-P. Zheng, "The neuromotor effects of transverse friction massage," *Man. Ther.* **26**, 70–76 (2016).
- <sup>18</sup>S. J. Brull, J. Ehrenwerth, and D. G. Silverman, "Stimulation with sub-maximal current for train-of-four monitoring," *Anesthesiology* **72**(4), 629–632 (1990).
- <sup>19</sup>H. K. Cheng and A. G. Schwing, "XMem: Long-Term video object segmentation with an Atkinson–Shiffrin memory model," in *Computer Vision – ECCV 2022*, edited by S. Avidan, G. Brostow, M. Cissé, G. M. Farinella, and T. Hassner (Springer Nature, Switzerland, Cham, 2022), pp. 640–658.
- <sup>20</sup>S. W. Oh, J.-Y. Lee, N. Xu, and S. J. Kim, "Video object segmentation using space-time memory networks," in *Proceedings of the IEEE/CVF International Conference on Computer Vision (IEEE, 2019)*, pp. 9226–9235.
- <sup>21</sup>J. Pont-Tuset, F. Perazzi, S. Caelles, P. Arbeláez, A. Sorkine-Hornung, and L. Van Gool, "The 2017 DAVIS challenge on video object segmentation," *arXiv:1704.00675* (2017).
- <sup>22</sup>H. Carvalho, M. Verdonck, W. Cools, L. Geerts, P. Forget, and J. Poelaert, "Forty years of neuromuscular monitoring and postoperative residual curarisation: A meta-analysis and evaluation of confidence in network meta-analysis," *Br. J. Anaesth.* **125**(4), 466–482 (2020).
- <sup>23</sup>G. Giudici, F. Piccioni, P. Proto, and F. Valenza, "A comparison of accelerometric monitoring by TOF watch<sup>®</sup> SX and electromyographic monitoring by tetragraph<sup>®</sup> for recovery from neuromuscular blockade," *J. Clin. Anesth.* **75**, 110481 (2021).
- <sup>24</sup>S. S. Liang, P. A. Stewart, and S. Phillips, "An ipsilateral comparison of acceleromyography and electromyography during recovery from nondepolarizing neuromuscular block under general anesthesia in humans," *Anesth. Analg.* **117**(2), 373 (2013).
- <sup>25</sup>Z. Wedemeyer, S. Jelacic, K. Michaelsen, W. Silliman, K. Togashi, and A. Bowdle, "Comparative performance of stimpod electromyography with mechanomyography for quantitative neuromuscular blockade monitoring," *J. Clin. Monit. Comput.* **38**(1), 205–212 (2024).